Materials Science-Poland, *Vol. 26*, *No. 2*, *2008*

Nickel-free nanocrystalline austenitic stainless steels

M. TULINSKI[1*], K. JURCZYK[2], M. JURCZYK[1]

[1]Poznań University of Technology, Institute of Materials Science and Engineering,
ul. M. Skłodowskiej-Curie 5, 60-965 Poznań, Poland

[2]Poznań University of Medical Sciences, Department of Conservative Dentistry and Periodontology,
ul. Bukowska 70, 60-812 Poznań, Poland

Nanocrystalline Ni-free austenitic stainless steel powders have been synthesised by mechanical alloying followed by nitrogenation. Phase transformation from ferritic to austenitic phases was confirmed by the XRD analysis. After mechanical alloying microhardness reached the values almost twice higher than those of materials obtained by conventional methods. The effect is directly connected with the structure refinement. The results of the corrosion resistance showed that mechanical alloying process and nitrogen absorption treatment significantly lowered corrosion rates.

Key words: *Ni-free stainless steel; mechanical alloying; biomaterials*

1. Introduction

Microcrystalline materials such as metals and alloys are widely used today. Over the last decade, the use of nanostructured materials has already changed the approach to designing materials in many applications by seeking structural control at the atomic level and tailoring mechanical engineering properties [1].

Today, it is possible to prepare metal/alloy nanocrystals with nearly monodispersive size distribution. Nanostructures represent key building blocks for nanoscale science and technology. They are needed to implement the "bottom-up" approach to nanoscale fabrication, whereby well-defined nanostructures with unique properties are assembled into mechanical as well as functional properties [2].

One of the potential applications of nanostructured materials (made of elements of the size not exceeding 100 nm) is medicine. Presently, most biomedical implants, e.g. stents, contain stainless steel frameworks. However, widely used 316L steel is not fully biocompatible, and has induced high occurrences of restenosis and thrombosis.

[*]Corresponding author, e-mail: maciej.tulinski@doctorate.put.poznan.pl

Moreover, nickel ions produced due to corrosion are reported to cause allergies and even cancer. Scientists have therefore been searching for more biocompatible options which include gold, titanium, cobalt-chromium alloys, tantalum alloys and various polymers.

Mechanical and corrosion resistance properties of typical metallic biomaterials used for implant devices are satisfactory but they may cause many problems within human body and therefore need improvement. The main disadvantage of the most popular austenitic stainless steel (316L) [3] is lack of biocompatibility, toxicity of corrosion products and fracture due to corrosion fatigue [4]. Austenite stabilizer – nickel – is reported to be a particularly toxic element causing allergies and even cancer [5]. World Health Organization (WHO) estimated that nickel content below 0.2% is congruous with medical requirements [4]. Therefore, development of materials with either improved corrosion resistance and/or without nickel is absolutely imperative.

One of the most promising austenitizing elements to replace nickel is nitrogen [6]. Nitrogen increases austenite stability, corrosion resistance and prevents from the formation of sigma phase. Recently, a new manufacturing process of nickel-free austenitic stainless steels with nitrogen absorption treatment has been developed [7]. In this method, small devices can be precisely machined in a ferritic phase and then during nitrogenization of their surfaces under gaseous nitrogen at ca. 1200 ºC they become nickel-free austenitic stainles steels with better mechanical and corrosion resistance properties.

In this work, a new manufacturing process of nickel-free austenitic stainless steels with nanostructure has beed proposed. Details of the process and the enhancement of properties due to obtaining nanostructure in consolidated materials are presented.

2. Experimental

The experimental procedures are shown in Fig. 1. Mechanical alloying (MA) was developed in the 1970's at the International Nickel Co. as a technique for dispersing nanosized inclusions into nickel-based alloys [1]. During the last years, the MA process has been successfully used to fabricate a variety of alloy powders including powders containing supersaturated solid solutions, quasicrystals, amorphous phases and nano-intermetallic compounds. MA technique has been proved to be a novel and promising method for alloy formation.

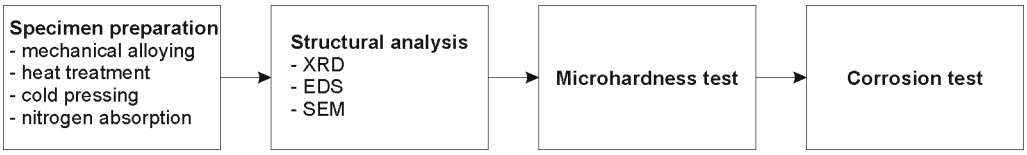

Fig. 1. Flow chart of the experiment

Raw materials used for MA are commercially available as high purity powders that have sizes in the range of 1–100 μm. During the mechanical alloying process, the powder particles are periodically trapped between colliding balls and are plastically

deformed due to generation of a wide number of dislocations as well as other lattice defects. Furthermore, the ball collisions cause fracturing and cold welding of elementary particles, forming clean interfaces at the atomic scale. Further milling results in a decrease of sizes of elementary components from millimeter to submicrometer lengths, thus increasing the number of interfaces. Concurrently to this decrease of the elementary distribution, some nanocrystalline intermediate phases are produced inside the particles or at their surfaces. As the milling develops, the content fraction of such intermediate compounds increases leading to a final product whose properties depend on the milling conditions.

The FeCrMnMoN alloys were prepared by mechanical alloying of stoichiometric amounts of the constituent elements (99.9% or better purity). The mechanical alloying was carried out using a SPEX 8000 mixer mill fitted with a hardened steel vial and steel balls 10 mm in diameter. The vial of the SPEX mill was loaded with powder in a glove-box connected to a high purity argon supply. The elemental powders (Fe 10 μm, Cr 5 μm, Mn 44 μm, Mo 10 μm) were mixed and poured into the vial (Fig. 2a). The mill was run up to 48 h for every powder preparation (Fig. 2b). The as-milled powders were heat treated at 750 ºC for 0.5 h under high purity argon to form ordered phases (Fig. 2c). Nitrogenation of cold pressed samples was carried out at 1215 ºC for 24 h at 120 kPa nitrogen pressure (Fig. 2e).

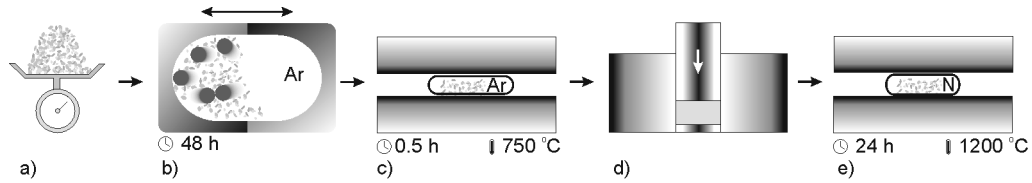

Fig. 2. Schematic presentation of manufacturing of nanocrystalline stainless steels: a) initial powders, b) mechanical alloying, c) heat treatment, d) cold pressing, e) nitrogen absorption

The powders were characterized by means of X-ray diffraction (XRD) and scanning electron microscopy (SEM) with an energy-dispersive X-ray microanalysis system (EDS). XRD was performed using an X-ray powder diffractometer with CoK_{α} radiation at various stages during milling, prior to annealing and after annealing as well as after nitrogenation. Microhardness measurements were carried out using the Vickers method with the load of 200 g. The micrographs were obtained using an optical microscope. The density of the sintered samples was determined by the Archimedes method. The analyses of the corrosion were conducted on a Solartron 1285 potentiostat in a Princeton Applied Research corrosion cell system interfaced to a personal computer. The experiments were controlled and the data were analyzed using a CorrWare analysis software. Counter electrodes were made of graphite, the reference electrode was a standard calomel electrode (SCE). The method of polarization resistance was employed to investigate changes in corrosion. The etching solution was 0.1 M H_2SO_4. Scanning range extended from –1 V to 2.5 V with the rate of 0.5 mV/s. All

experiments were carried out at 25 ºC. From the analyses, the corrosion currents, I_{corr}, were recorded. The corrosion rate (MPY) can be then calculated as follows:

$$MPY = \frac{0.00408 I_{corr} A}{nD} \tag{1}$$

where I_{corr} is the corrosion current (A/cm^2), D is the density (7.8 g/cm^3 for stainless steel) and A/n is the effective weight (25.29 g).

The steel specimens were used in the form of rods 8 mm in diameter and 3 mm long. They were prepared and mounted as follows. A stainless steel rod 200 mm long and 3.5 mm diameter was used for establishing the electrical contact. The whole assembly was inserted in a glass tube. Silicon resin was used to ensure the exposure of a determined apparent surface area of 0.5 cm^2.

3. Results and discussion

X-Ray diffraction patterns in Fig. 3 are representative of a $Fe_{74}Cr_{24}Mo_2$ alloy after MA, annealing and nitrogenation under various conditions. The first diffraction pattern

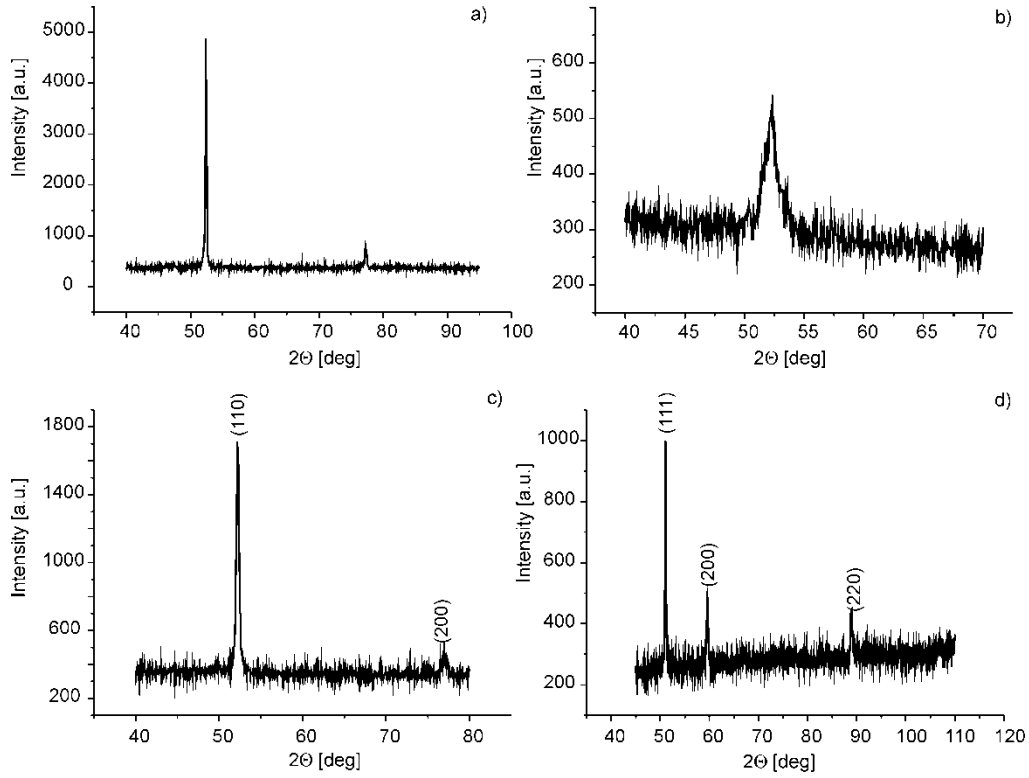

Fig. 3. X-ray diffraction spectra of $Fe_{74}Cr_{24}Mo_2$ material: a) mixture of initial powders, b) after 48 h of mechanical alloying, c) after heat treatment at 750 ºC for 0.5 h, d) after nitrogen absorption

shows a mixture of initial powders (Fig. 3a). After 48 h of MA the alloy decomposed into an amorphous phase and nanocrystalline α-Fe (Fig. 3b). The heat treatment performed after MA resulted in crystallization into ferritic phase (Fig. 3c). Then the compacted material was nitrided at 1215 ºC which resulted in phase transformation from ferritic phase to fully austenitic one (Fig. 3d). Crystallite size of the material, 27 nm, was estimated by Scherrer's method. Some small peaks might indicate a possibility of a presence of small amounts of nitrides or oxides as results from the chemical composition (Fig. 4).

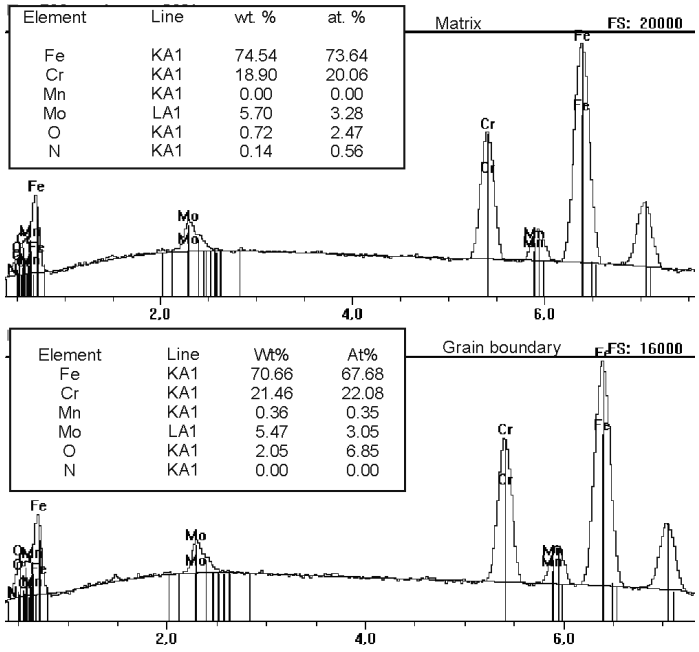

Fig. 4. EDX analysis of the matrix and at the grain boundary of $Fe_{74}Cr_{24}Mo_2$ sample

EDX analysis (Fig. 4) of $Fe_{74}Cr_{24}Mo_2$ alloy confirms that the material matrix contains 74% of iron, 20% of chromium and 3% of molybdenum, 0.56% of nitrogen and 2.47% of oxygen. Oxygen content in the syntesized materials was determined by the XPS method. At the grain boundaries one can observe a small amount of manganese and an increase of oxygen content up to 7%. Nitrogen content is dependent on the region, ranging from 0 to 2.16% due to diffusion effects.

Sizes and shapes of microcrystals of mechanically alloyed powder mixtures during MA have been determined by the SEM technique (Fig. 5). Starting materials forming the microstructure (Fig. 5a–5c) were mixed together (Fig. 5d). The lamellar structure is increasingly refined during further mechanical alloying (Fig. 5e) which leads to formation of solid solution (Fig. 5f). After alloying, the samples show cleavage fracture morphology and inhomogeneous size distribution (Fig. 5g).

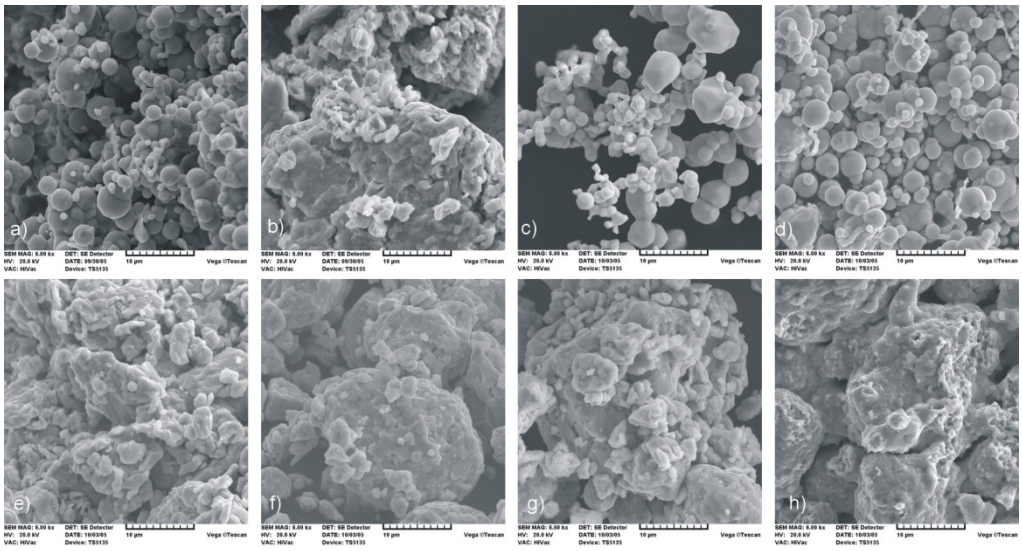

Fig. 5. SEM images: a) Fe, b) Cr, c) Mo, d) mixture of initial powders, e) after 1 h of MA, f) after 48 h of MA, g) after heat treatment, h) final bulk material $Fe_{74}Cr_{24}Mo_2$ after nitrogen absorption

Many small powder particles tend to agglomerate. Bulk FeCrMo material with 98% theoretical density was prepared by sintering (750 ºC for 0.5 h) and then nitrided at 1215 ºC for 24 h (Fig. 5h).

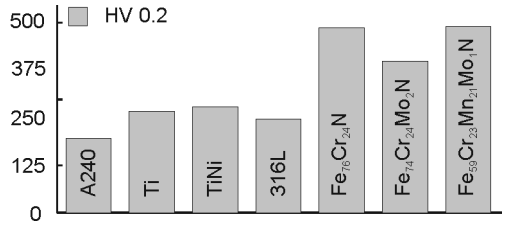

Fig. 6. Microhardness of FeCrMoN materials compared to A240 and 316L stainless steels, pure titanium and microcrystalline TiNi alloy

The microhardness of the final bulk material was studied using the Vickers method (Fig. 6). Compared with A240 commercial austenitic stainless steel (195 $HV_{0.2}$), pure titanium (266 $HV_{0.2}$), TiNi alloy (279 $HV_{0.2}$) and widely used in medicine 316L stainless steel (248 $HV_{0.2}$), microhardness of sintered nanocrystalline austenitic nickel-free nitrogen containing stainless steels obtained by mechanical alloying is significantly higher (378 to 487 $HV_{0.2}$) being twice higher than microhardness of austenitic steel obtained by conventional methods. This effect is directly connected with structure refinement and obtained nanostructure, one should, however, consider also change in the phase composition since small peaks in the X-ray diffraction patterns might indicate a possibility of formation of oxides and nitride. Due to its small amount it is of lesser importance.

General shapes of the potentiodynamic curves are shown in Fig. 7. Results of the corrosion test are listed in Table 1. The linear parts of anodic and cathodic Tafel re-

gions extended over a wider current range in the case of $Fe_{59}Cr_{23}Mn_{12}Mo_6$. The calculated corrosion potential, E_{corr}, in the case of $Fe_{59}Cr_{23}Mn_{12}Mo_6$ is –431 mV with an associated corrosion current, I_{corr}, of 1.3×10^{-5} A/cm^2. The corresponding values in $Fe_{74}Cr_{24}Mo_2$ are –473 mV and 6.1×10^{-3} A/cm^2, respectively. Thus the addition of Mn and a decrease of the Fe content resulted in the shift of the corrosion potential to a more negative value and appreciable (two orders of magnitude) decrease in the corrosion current density. The values for $Fe_{74}Cr_{24}Mo_2$ are similar as those for 316L stainless steel widely used in medicine while those for $Fe_{59}Cr_{23}Mn_{12}Mo_6$ are considerably improved.

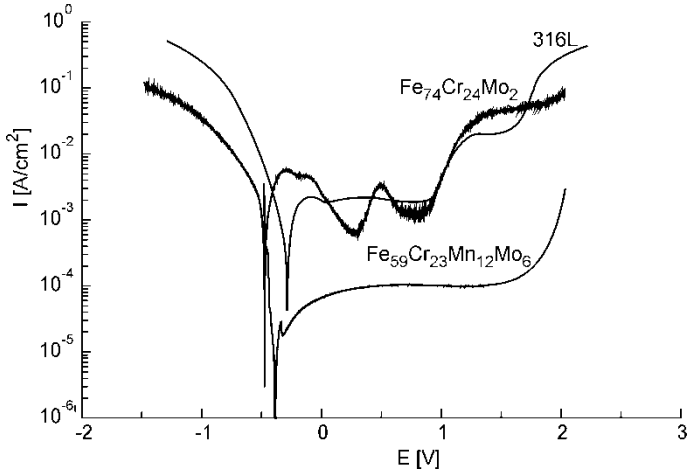

Fig. 7. Potentiodynamic curves for stainless steels in 0.1 M H_2SO_4 at 25 ºC

The potentiodynamic curve was characterized by the appearance of a well-defined anodic peak at –350 mV, which corresponds to an anodic peak current of 6.2×10^{-4} A/cm^2 for $Fe_{59}Cr_{23}Mn_{12}Mo_6$. On the other hand, the corresponding values for $Fe_{74}Cr_{24}Mo_2$ are –280 mV and 5.3×10^{-2} A/cm^2, respectively.

Table 1. Results of corrosion tests

Chemical composition	I_{corr} [A/cm^2]	E_{corr} [mV]	R_p [ohm/cm^2]	Corrosion rate [MPY]
$Fe_{74}Cr_{24}Mo_2$	6.1×10^{-3}	–473	22	47
$Fe_{59}Cr_{23}Mn_{12}Mo_6$	1.3×10^{-5}	–431	1500	7.4
316L	3.6×10^{-3}	–349	450	33

The polarization resistances R_p calculated from the potentiodynamic curves were 1.467×10^3 and 22 Ohm/cm^2 for $Fe_{59}Cr_{23}Mn_{12}Mo_6$ and $Fe_{74}Cr_{24}Mo_2$, respectively. The corresponding calculated corrosion rates are 7.4 and 47 MPY (milliinch per year),

respectively, resulting in lowering by ca. 85% of the rate of corrosion of the stainless steel in the 0.1 M H_2SO_4 solution.

4. Summary

Nanocrystalline austenitic nickel-free nitrogen containing stainless steel samples were produced by mechanical alloying process and nitrogen absorption. Microhardness test showed that the obtained material exhibits the Vickers microhardness as high as 487 $HV_{0.2}$ being about two times higher than that of conventional austenitic stainless steels, including widely used in medicine 316L stainless steel. This effect might be smaller when considering possibility of presence of nitride. This is due to the structure refinement and the transformation into nanostructured material. Mechanical alloying is also a very effective technology to improve the corrosion resistance of stainless steel. Decreasing the corrosion current density is a distinct advantage for prevention of ion release. According to existing concepts, decreasing size of material crystallites to a nanometric scale allows one to achieve much better mechanical properties (e.g. microhardness) compared to conventional materials.

Nitrogen absorption treatment contributes to a higher corrosion resistance, also in the presence of wear. With regard to austenitic stainless steels this may lead to obtaining biomedical implants (e.g., stents) with better mechanical properties, corrosion resistance and biocompatibility.

References

[1] GLEITER H., Prog. Mater. Sci., 33 (1989), 323.
[2] JURCZYK M., Bull. Pol. Ac. Tech., 52 (2004), 67.
[3] LIM I.A.L., MIT Undergraduate Res. J., 11 (2004), 3.
[4] IARC Monographs on the Evaluation of Carcinogenic Risks to Humans: *Surgical Implants and Other Foreign Bodies*, Lyon, 74 (1999), 65.
[5] UGGOWITZER J., MAGDOWSKI R., SPEIDEL M., ISIJ Int., 36 (1996), 901.
[6] ORNHAGEN C., NILSSON J.O., VANNEVIK H., J. Biomed. Mater. Res., 31 (1996), 97.
[7] SUMITA M., HANAWA T., TEOH S.H., Mater. Sci. Eng. C, 24 (2004), 753.

Received 28 April 2007
Revised 16 February 2008